Clinico-Radiological-Pathological Correlation of Visual Loss in COVID-Associated Rhino-Orbito-Cerebral Mucormycosis

Ruchi Goel, M.S., D.N.B., F.R.C.OPTH, Ritu Arora, M.D., D.N.B., F.R.C.OPTH*, Shalin Shah, M.B.B.S., M.R.C.S.ED*, Mohit Chhabra, M.S., D.N.B.*, Jyoti Kumar, M.D.*, Nita Khurana, M.D.‡, Swati Gupta, M.D., D.N.B., F.R.C.R.†, Samreen Khanam, M.S., D.N.B.*, Sumit Kumar, M.S.*, Sonam Singh, M.B.B.S.*, Ravi Meher, M.S.§, Meenakshi Thakar, M.D., F.R.C.S.ED*, and Anju Garg, M.D.†*

**Department of Ophthalmology (Guru Nanak Eye Centre), Maulana Azad Medical College, New Delhi, India; †Department of Radiodiagnosis, Maulana Azad Medical College, New Delhi, India; ‡Department of Pathology, Maulana Azad Medical College, New Delhi, India; §Department of Otorhinolaryngology, Maulana Azad Medical College, New Delhi, India*

Purpose: To correlate the clinical, radiological, and histopathological features in Covid-associated Rhino-orbito-cerebral mucormycosis cases presenting with acute visual loss.

Design: Cross-sectional study.

Methods: Covid-associated Rhino-orbito-cerebral mucormycosis cases with unilateral visual loss, planned for exenteration, underwent orbital and ophthalmological ocular examination. The available radiological sequences, doppler ultrasonography and histopathology findings were correlated with clinical manifestations.

Results: The median age was 51 years and the male: female ratio was 3:1. All except one presented with unilateral ophthalmoplegia. The ocular media were hazy in 2 eyes. In 8 eyes, retinal changes were suggestive of occlusion of CRA (6), combined occlusion of CRA and central retinal vein (1), and myopic degeneration with hypertensive retinopathy (1). The contralateral eye showed retinal ischemic changes in one patient. Radiological imaging showed orbital apex involvement in the 10 affected eyes and one contralateral eye. Ipsilateral cavernous sinus thrombosis, diffusion restriction on MRI of optic nerve, internal carotid artery narrowing/thrombosis, and cortical watershed infarcts were seen in 8, 4, 4, and 2 cases, respectively. The blood flow in CRA and ophthalmic artery was absent or reduced in all the 10 affected eyes and in 1 contralateral eye. On histopathology, orbital fat necrosis, fungal hyphae, acute inflammation, granuloma formation, ischemic thrombosis of ophthalmic artery was observed in 10 specimens. CRA was patent in 9 and thrombosed in 1 eye. Optic nerve was ischemic in 8 and viable in 2 eyes.

Conclusion: Acute visual loss in ROCM cases is associated with orbital apex involvement and thrombotic ischemia of ophthalmic artery. Cessation of flow in CRA possibly occurs secondary to ophthalmic artery thrombosis.

(*Ophthalmic Plast Reconstr Surg* 2022;38:242–249)

Rhino-orbito-cerebral mucormycosis (ROCM) is a life-threatening condition caused by fungi of the order Mucorales.[1] Recently, India witnessed an epidemic of ROCM cases following infection with SARS CoV-2. The reported primary symptoms in a multicentric study of 2716 COVID-associated ROCM patients were orbital/facial pain (23%), orbital/facial edema (21%), loss of vision (19%), ptosis (11%), nasal obstruction (9%), proptosis (6.5%), nasal discharge (6%), diplopia (2%), headache (0.9%), orbital/facial discoloration (0.8%), toothache (0.7%), loose teeth (0.1%), epistaxis (0.1%), and facial palsy (0.1%).[2]

The fungus, with its ability to adhere and to invade the endothelium of blood vessels, results in thrombus formation in the cavernous sinus, internal carotid artery (ICA), ophthalmic artery (OA), central retinal artery (CRA), or posterior ciliary arteries.[3–6] Besides the direct spread, ICA may be invaded through retrograde extension from OA. Thrombosis of ophthalmic vessels can thus be a predictor of subsequent development of cerebral infarcts.[7,8]

Orbital involvement in mucormycosis occurs through the medial orbital wall, inferior orbital fissure, nasolacrimal duct, or by angioinvasion leading to vascular occlusion. The visual loss may be consequent to external compression of optic nerve at the orbital apex or luminal invasion of ocular blood vessels by the fungus.[2]

The study was conducted to correlate clinical, radiological, and histopathological findings of patients with visual loss in ROCM cases. To the best of our knowledge, this is the first clinico-radiological-pathological study of acute blindness in COVID-19-associated mucormycosis.

MATERIALS AND METHODS

A non-randomized cross-sectional study was conducted after obtaining institutional ethical committee clearance (F.1/IEC/MAMC/88/02/2021/No.384 dated 27/05/21) according to tenents of Helsinki as amended in 2013. Ten patients of ROCM, with acute loss of light perception in one eye, planned for exenteration, admitted into the mucormycosis ward of a large tertiary care hospital center, were enrolled for the study after obtaining written informed consent from June 1 to July 31, 2021. Only patients with positive RT-PCR of nasopharyngeal swab for SARS-CoV-2 within the preceding 3 months, currently negative, were included. They were being treated with intravenous amphotericin B liposomal (Amphonex-Bharat serums and vaccines ltd) (IV 5mg/kg daily) and had undergone functional endoscopic sinus surgery, in the preceding 2 weeks or were scheduled for debridement.Critically ill patients unable to give consent were excluded from the study.

Accepted for publication October 28, 2021.

The authors have no financial or conflicts of interest to disclose.

Address correspondence and reprint requests to Ruchi Goel, M.S., D.N.B., F.R.C.Opth, Department of Ophthalmology. Guru Nanak Eye Centre, Maulana Azad Medical College, New Delhi 110002, India. E-mail: gruchi1@rediffmail.cynom

DOI: 10.1097/IOP.0000000000002112

TABLE. Clinical, radiological, and histopathological findings of the affected eye

					Structures evaluated on radiological imaging							Doppler (PSV) cm/s		Histopathology			
Sr No	Age (years)	Sex	Fundus findings	Imaging modality	ICA	OA	CS thrombosis	Brain	Orbital apex involvement	Loss of contrast enhancement of orbital tissues	Diffusion restriction of optic nerve	OA	CRA	OA	CRA	Orbital apex disease	Optic nerve
1	51	M	Media hazy due to old uveitis	MR-DWI	Narrow	Not visualized	Present	Normal	Present	Present	Present	0	0	Ischemic thrombosis	Patent	Present	Ischaemia
2	76	F	Myopic degeneration, hypertensive retinopathy	CECT	Normal	Not visualized	Present	Normal	Present	Not visualized	Not visualized	5.76	0	Ischemic thrombosis	Patent	Present	Ischaemia
3	61	M	CRAO	MR-DWI-TOF angiography	Thrombosed	Thrombosed	Present	Watershed infarcts in ACA/MCA and MCA/PCA waterbed	Present	Present	Absent	0	0	Ischemic thrombosis	Patent	Present	Ischaemia
4	50	F	Media hazy due to orbital infarction syndrome	MR-DWI	Narrow	Not visualized	Present	Normal	Present	Present	Absent	0	0	Ischemic thrombosis	Ischaemic thrombosis	Present	Ischaemia
5	71	M	CRAO	MR-DWI-TOF Angiography	Normal	Thrombosed	Absent	Normal	Present	Present	Present	0	0	Ischemic thrombosis	Patent	Present	Ischaemia
6	32	M	CRAO	MR-DWI	Normal	Not visualized	Absent	Frontal lobe abscess	Present	Present	Present	8.83	0	Ischemic thrombosis	Patent	Present	Ischaemia
7	50	M	CRAO	MR-DWI	Narrow	Not visualized	Present	Normal	Present	Present	Present	9.6	0	Ischemic thrombosis	Patent	Present	Ischaemia
8	34	F	CRAO	MR-DWI-TOF Angiography	Thrombosed	Thrombosed	Present	Watershed infarcts in MCA/PCA waterbed	Present	Present	Absent	8.35	0	Ischemic thrombosis	Patent	Present	Viable
9	48	M	CRAO+CRVO+disc edema	CECT	Normal	Not visualized	Present	Normal	Present	Not visualized	Not visualized	0	0	Ischemic thrombosis	Patent	Present	Ischaemia
10	55	M	CRAO	MR-DWI	Narrow	Not visualized	Present	Normal	Present	Present	Absent	13.1	0	Ischemic thrombosis	Patent	Present	Viable

ACA, anterior cerebral artery; CECT, contrast-enhanced computerized tomography; CRA, central retinal artery; CRAO, central retinal artery occlusion; CS, cavernous sinus; F, female; ICA, internal carotid artery; M, male; MCA, middle cerebral artery; MR-DWI, magnetic resonance-diffusion-weighted imaging; OA, ophthalmic artery; PCA, posterior cerebral artery; PSV, peak systolic velocity; TOF, time of flight.

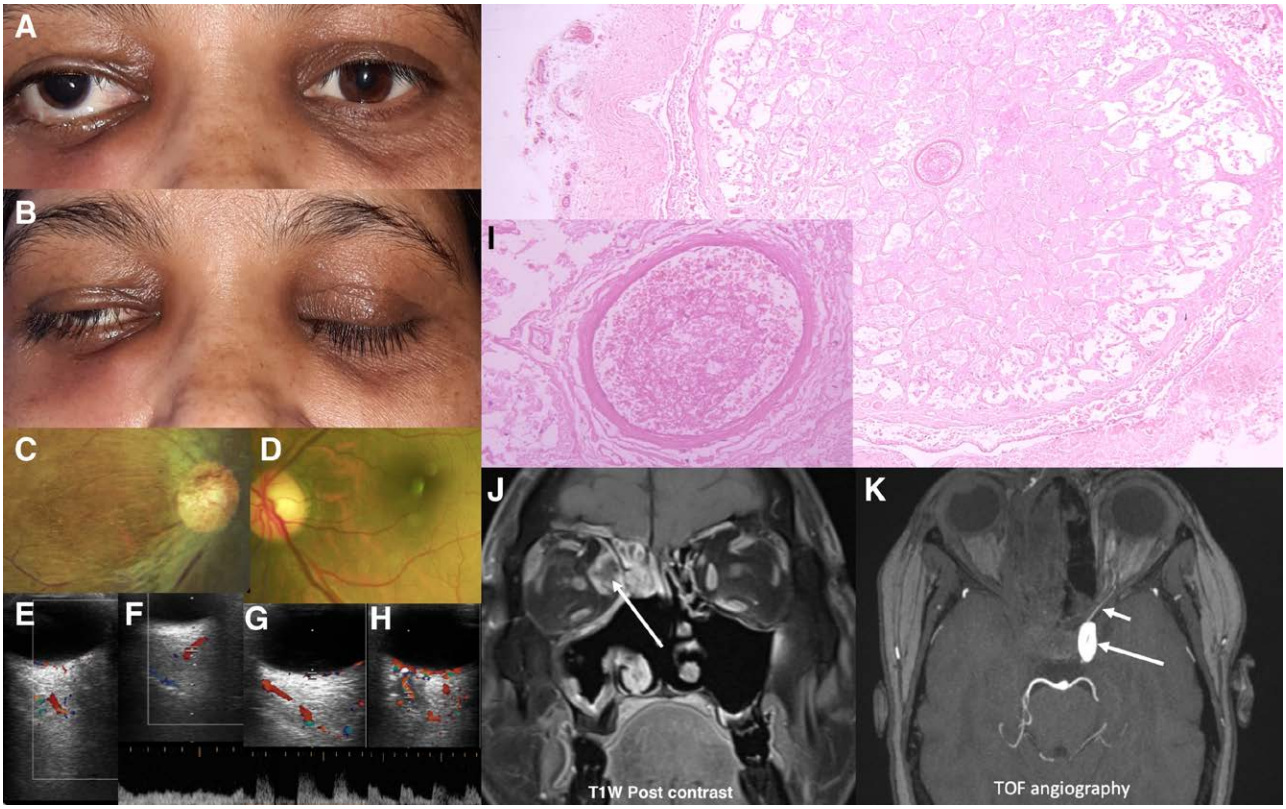

FIG. 1. Clinical photograph shows (**A**) right partial ophthalmoplegia with periorbital abscess. **B**, Right infranuclear facial palsy. Fundus photograph. **C**, Right eye central retinal artery occlusion in right eye. **D,** Normal left eye. Doppler ultrasonography with PSV of (**E**) 0 cm/s in right central retinal artery (CRA) (**F**) 8.35 cm/s in right ophthalmic artery (OA) (**G**) 12.1 cm/s in left CRA (**H**) 36.1 cm/s in left OA. **I**, Histopathology of right exenterated orbit depicts optic nerve ischemia with patent CRA showing red blood cells (inset) (HE, 40×). **J**, Coronal view of post contrast MRI shows right ethmoid sinus disease extending into the medial extraconal fat of right orbit seen as lack of contrast enhancement (marked with arrows). **K**, Time of flight (TOF) angiography image depicts nonvisualization of right internal carotid artery (ICA) as well as OA. Normal ICA and OA is seen on the left side (marked with arrows).

History was taken, and bedside examination was performed. Vision was recorded using Snellen's chart and fundus photographs were taken with smart phone and a +20D lens. Intraocular pressure was recorded using Schiotz tonometer. Radiological imaging such as contrast-enhanced computerized tomography or magnetic resonance imaging (CE-MRI) with diffusion-weighted imaging (DWI), whichever available, of the orbit and brain were analyzed to see the extent of orbital invasion and involvement of cavernous sinus. Hyperintensity of optic nerve on DWI and signal drop on ADC map (apparent diffusion coefficient) was considered to represent ischemic optic neuropathy. Magnetic resonance time of flight angiography images were utilized for studying the flow in ICA and OA.

Additionally, color doppler imaging of both eyes was performed to record the ophthalmic artery: peak systolic velocity (OA-PSV) and central retinal artery: peak systolic velocity (CRA-PSV) using 7.5 MHz linear probe (Philips Medical Systems, Best, The Netherlands). OA-PSV and CRA-PSV of 10 age-matched controls undergoing abdominal ultrasonography were also recorded after obtaining informed consent. None of the control group patients had a systemic disease that could influence vascular flow.

Histopathological sections of the exenterated orbit were evaluated using Periodic Acid Schiff and Silver methenamine staining.

RESULTS

The median age of the 10 study participants was 51 years (ranging 32–76 years), and the male:female ratio was 3:1. All were laboratory proven COVID positive on nasopharyngeal swab 15 to 35 days prior to diagnosis of mucormycosis. The severity of COVID-19 was mild in 6, moderate in 2, and severe in 2 patients. All the patients were diabetic, the median glycosylated hemoglobin on admission being 9.9 % (ranging from 7% to 14.3%). Other comorbidities were hypertension (7/10), coronary-artery-disease (3/10), and hypothyroidism (1/10). There were no smokers in the cohort.

The clinical, radiological, and pathological findings are given in Table and Figs. 1–5.

Findings on Clinical Examination. Bilateral ophthalmoplegia was found in a single patient. He had total ophthalmoplegia with absence of light perception in right eye and partial ophthalmoplegia with visual acuity of log MAR 0.2 in the left eye (case number 6). Unilateral orbital involvement with partial or total ophthalmoplegia, relative afferent pupillary defect, numbness of upper two-thirds of ipsilateral face in the affected eye was seen in the remaining 9 patients. Additionally, ipsilateral lower motor neurone facial nerve palsy was seen in one of these patients (case number 8) (Fig. 1B), and the best corrected visual acuity in the contralateral eye ranged from log MAR 0.0 to 0.3. There was no evidence of sensory or motor deficit elsewhere in the body in any of the patients.

Acute loss of vision was the presenting symptom of mucormycosis in 6 eyes, while vision loss developed 7 to 13 days after admission for management of mucormycosis in the remaining 4 eyes of 10 patients. Retinal changes were suggestive of central retinal artery

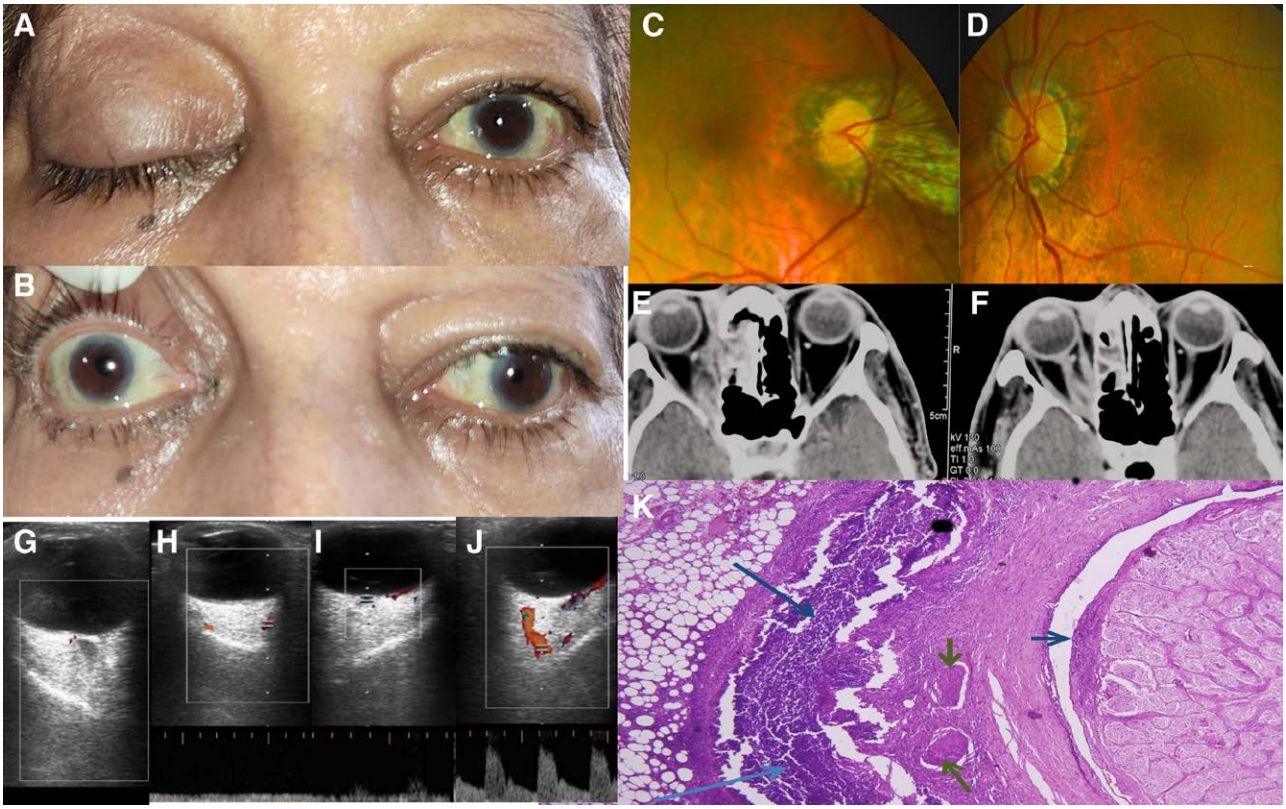

FIG. 2. Clinical photograph (**A**) severe ptosis in right eye (**B**) limitation of extraocular movements of right eye. Fundus image shows myopic retinal degeneration and hypertensive retinopathy in (**C**) right eye and (**D**) left eye. CT scan images show (**E**) disease extending from the right ethmoid sinus into the ipsilateral orbit with involvement of extraconal as well as intraconal compartment and (**F**) right lacrimal sac region is also involved. Doppler ultrasonography showing PSV of (**G**) 0 cm/s in right CRA (**H**) 5.76 cm/s in right ophthalmic artery (OA) (**I**) 10.1 cm/s in left CRA (**J**) 34.0 cm/s in left OA. **K**, Histopathology of right exenterated orbit shows dense inflammation in the orbital tissue (long blue arrows) focally extending in the optic nerve sheath (short blue arrow). Few nerve twigs entrapped in the inflammation (green arrows) (HE, 200x).

occlusion (CRAO) in 6 eyes (Fig. 1C and 5B) and combined central retinal vein (CRV) and CRA in 1 eye (case 9). Bilateral myopic degeneration with grade 2 hypertensive retinopathy in absence of any definitive sign of vascular occlusion was seen in case number 2 (Fig. 2C, D). In 2 eyes, the media were hazy in the affected eye. In one of these, there was no view of retina due to occlusio pupillae following chronic uveitis (Fig. 3B). In the other case, ischemic retina was hazily seen through an opalescent anterior chamber suggestive of orbital infarction syndrome (OIS) (Fig. 4H). The contralateral eye showed evidence of retinal ischemia in the form of cotton wool spots and arterial attenuation in case number 6 (Fig. 5C). In the remaining 8 patients, contralateral fundus appeared normal.

The intraocular pressure ranged from 14.6 to 20.6 mm of Hg in 19 eyes of 20 cases and was 10.2 mm of Hg in the affected eye of case 1 (Table).

Imaging findings on CT/ MRI (orbit and brain). Two patients had CE-CT and 8 had CE-MRI of the orbit and brain. Magnetic resonance time of flight angiography sequences were available in only 3 patients. Orbital apex was involved unilaterally in 9 cases and bilaterally in 1 patient (Fig. 5E, F). Ipsilateral cavernous sinus thrombosis was present in 8 cases. Diffusion restriction of optic nerve was seen in 4 of 8 DWI sequences (Fig. 5G, H). ICA narrowing or thrombosis (Fig. 1K) on affected side was seen in 6 cases and infarction in cortical watershed areas of Anterior cerebral artery/middle cerebral artery and middle cerebral artery/posterior cerebral artery was seen on the ipsilateral side in 2 cases.

Imaging Findings on Doppler Ultrasonography. The CRA-PSV was 0 in all the 10 affected eyes of 10 patients (Figs. 1E, 2G, 3H, 4E, 5I). The OA-PSV was 0 cm/s in 5 and had flow ranging from 5.76 to 13.1cm/s, in the remaining 5 eyes (Figs. 1F, 2H, 3I, 4F, 5J). The mean OA-PSV and CRA-PSV in age-matched controls was 33.06±4.30 and 12.71±3.34cm/s, respectively. The CRA-PSV (Figs. 1G, 2I, 3F, 4C) and OA-PSV (Figs. 1H, 2J, 3G, 4D) were normal in the contralateral nine eyes. In contralateral eye of case number 6, CRA-PSV was 8.11cm/s (Fig. 5K) and OA-PSV was 9.55cm/s (Fig. 5L).

Findings on Histopathology. On histopathology, extensive orbital fat necrosis with the presence of broad aseptate fungal hyphae, acute inflammation, granuloma formation, ischemic thrombosis of OA (Fig. 5D) was seen in all the ten specimens. CRA was patent in 9 cases (Fig. 1I). Ischemic thrombosis of CRA along with fungal invasion of ocular coats was seen in the eye with OIS (case number 4) (Fig. 4J,K). In eye with occlusio-pupillae, acute inflammation and necrosis was seen in all the ocular coats with only retinal pigment layer being identifiable (case number 1) (Fig. 3D). Optic nerve ischemia was observed in 8 of 10 cases (Fig. 1I), 2 being viable (case number 9 and 10).

DISCUSSION

The sudden onset blindness in ROCM has been histologically correlated with CRAO, OA necrosis, optic nerve infarction and direct optic nerve infection by mucormycosis.[9–11] Orbital extension of mucormycosis may involve the orbital apex.

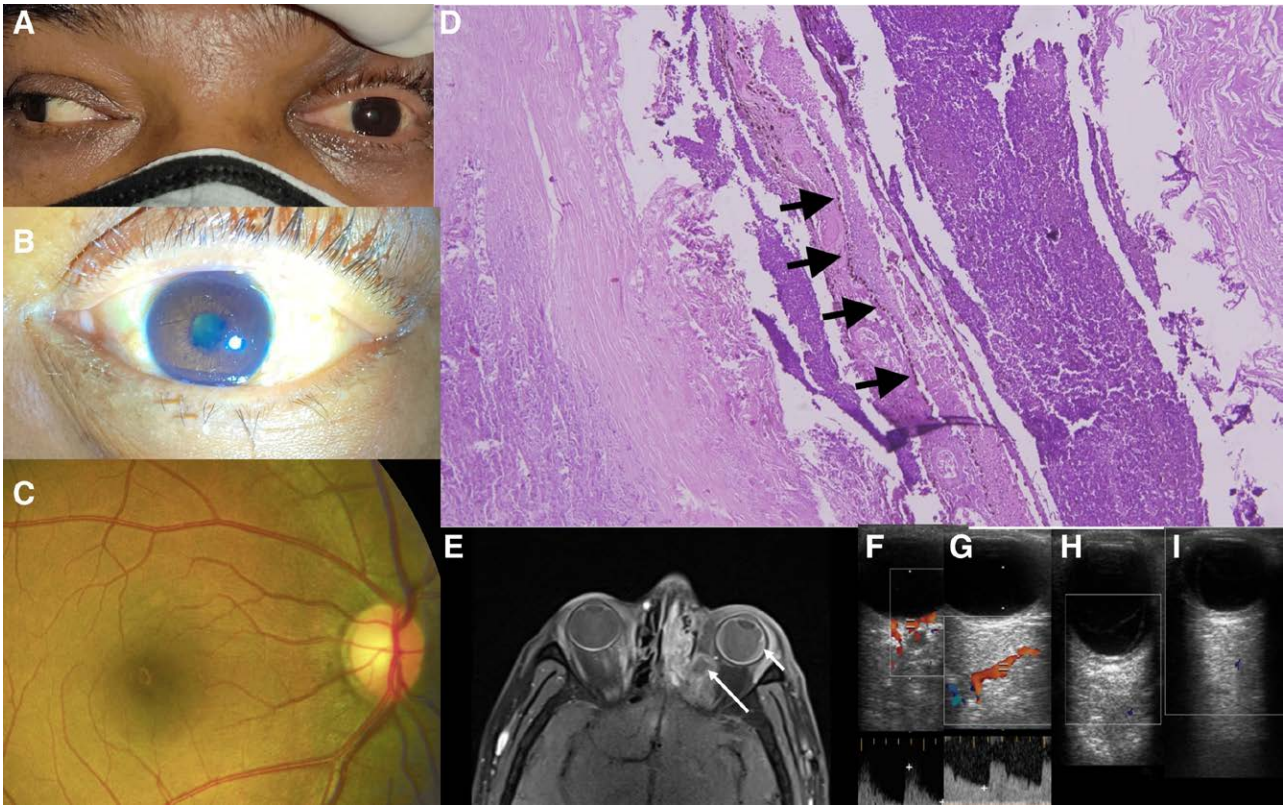

FIG. 3. **A**, Clinical photograph showing left total ophthalmoplegia. **B**, Left occlusion pupillae precluded retinal examination. **C**, Normal right fundus. **D**, Histopathology of left exenterated orbit shows acute inflammation and necrosis involving all ocular coats with only retinal pigment layer identifiable (black arrows) (HE, 40×). **E**, Postcontrast MRI shows left ethmoidal sinusitis with intra-orbital extension and area of lack of contrast enhancement within (long arrow) and left choroidal detachment (short arrow). Peak systolic velocity on doppler ultrasonography (**F**) 12.6 cm/s in right central retinal artery (CRA), (**G**) 30.6 cm/s in right ophthalmic artery (OA), (**H**) 0 cm/s in left CRA, (**I**) 0 cm/s in left OA.

The origin of the 4 recti muscles, optic nerve, ophthalmic artery, oculomotor nerve, abducens nerve and the nasociliary nerve are in close proximity in the apical region of the orbit. Thus the orbital apex syndrome results in visual loss of varying degree, ptosis, proptosis, total internal and external ophthalmoplegia and neuralgia of the ophthalmic nerve.[12,13] Also, angioinvasion of the wall of OA, CRA, or posterior ciliary artery can lead to ischemic infarction of optic nerve and retina.[14] Ischemia of the optic nerve may be a consequence of edema of the optic nerve in the optic canal due to compression of pial vascular plexus, supplied by branches of CRA, OA, and choroidal arteries.[15] In our series, the constellation of clinical signs was suggestive of mucormycosis-related orbital apex involvement, unilateral in 9 and bilateral in 1 patient.

The presenting visual acuity in acute CRAO (central retinal artery occlusion) ranges from log MAR 1.00 to counting fingers in absence of cilioretinal artery and hand motions or worse in ophthalmic artery occlusion.[16] There was loss of light perception in 10 eyes of 10 patients suggestive of ophthalmic artery occlusion in our study.

The typical fundus changes of acute CRAO are cherry red spot, posterior pole retinal opacity, box-car appearance of retinal arteries and veins, retinal arterial attenuation, optic disc edema, and optic disc pallor. Cherry red spot may not be detected in ophthalmic artery occlusion and in late stages of CRAO. In combined central retinal artery and venous vascular occlusion, the fundus exam shows superficial retinal whitening with cherry red spot and signs of venous obstruction, such as dilated, tortuous veins, intraretinal hemorrhages, optic disk edema, cotton wool spots, and marked retinal thickening.[16] Fundus findings in the study subjects were suggestive of CRAO in 6 eyes and combined CRAO with CRVO in 1 eye. There was no sign of vascular occlusion in 1 patient and in 2 eyes, fundus details were not visible. CRA-PSV was 0 and OA-PSV was either 0 or reduced in all the 10 affected eyes. In the patient with bilateral disease, in the contralateral left eye, fundus findings suggestive of retinal ischemia were seen and both OA-PSV and CRA-PSV were reduced. On MRI, there was extraconal and intraconal extension of disease in both orbits extending posteriorly to the orbital apices, right orbit more severely affected than the left. In addition, diffusion restriction of right optic nerve was seen (case number 6).

Ischemic thrombosis of OA was seen in all the 10 exenterated eyes, also evident in the 3 available magnetic resonance time of flight angiograms. Though CRA-PSV was 0 on doppler, the lumen was patent in 9 eyes on histopathology, the probable cessation of blood flow having occurred following thrombosis of OA. Only 1 eye, having fungal invasion of ocular coats showed ischemic thrombosis of CRA on histopathology (case number 4). These findings indicate that thrombosis of OA led to compromised blood flow in OA, which after reaching a critical level resulted in complete cessation of blood flow in CRA.

Optic nerve hyperintensity on DWI has been used as an indicator of traumatic optic neuropathy with 27.6% sensitivity (95% CI, 12.8%–47.2%) and 100% specificity (95% CI, 87.9%–100%).[17] DWI sequences available in 8 cases showed

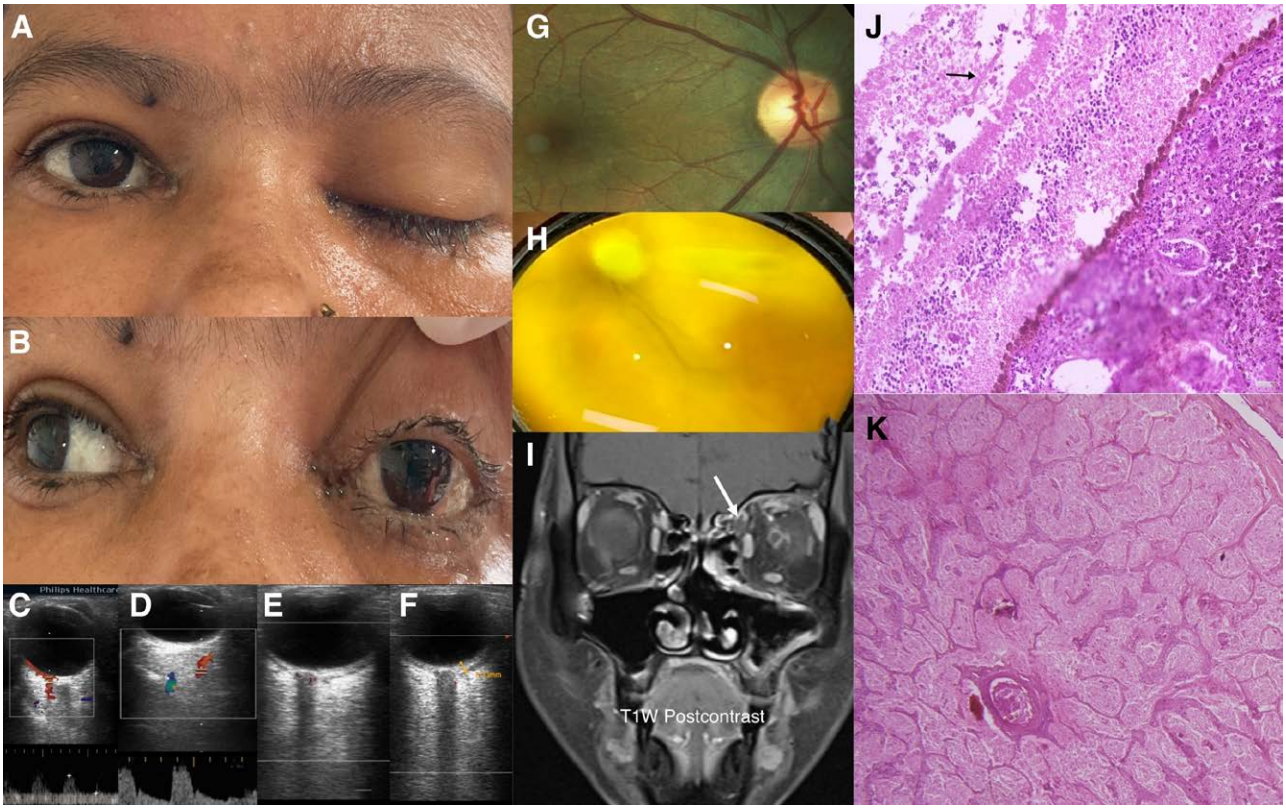

FIG. 4. Clinical photograph showing (**A**) severe ptosis in left eye, (**B**) limitation of extraocular movements of left eye. Doppler ultrasonography with peak systolic velocity of (**C**) 9.7 cm/s in right central retinal artery (CRA) (**D**) 30.4 cm/s in right ophthalmic artery (OA) (**E**) 0 cm/s in left CRA (**F**) 0 cm/s in left OA. Fundus photography showing (**G**) normal right eye, (**H**) ischemic retina seen through hazy media in left eye. **I**, Postcontrast T1-weighted coronal MRI shows a small focus of lack of enhancement within the left superior oblique muscle (white arrow). **J**, Retinal necrosis with entrapped fungal hyphae (black arrow) in the choroid and retina (HE, 200×), **K**, Early thrombus in CRA (HE, 100×).

diffusion restriction of optic nerve in 4 of the 8 affected eyes, corroborating with ischemic necrosis on histopathology. In the remaining 4 eyes lacking diffusion restriction of optic nerve, on histopathology, 2 were viable and 2 had ischemic necrosis.

MRI has been reported to be more sensitive than CT in detecting mucormycosis.[18,19] Loss of contrast enhancement of orbital tissue represents the presence of necrotic, unsalvageable nidus of fungal elements mandating debridement.[20] The general management principles of ROCM include initiation of systemic antifungals, endoscopic debridement of necrotic sinonasal tissue, and reduction of immune suppression. A working algorithm proposes retrobulbar transcutaneous amphotericin B administration in diffuse or apical enhancement and exenteration in absence of enhancement following administration of contrast.[21,22] Loss of contrast enhancement of tissues at orbital apex was seen in all 8 MRI sequences. In 2 cases where only CT scan was available, the decision to exenterate was based on clinical, doppler, and CT findings.

OIS is caused by ocular hypoperfusion due to stenosis of ≥90% of ipsilateral common or internal carotid and rarely OA.[23] Patients with well developed collateral circulation between internal and external carotid arteries or between the 2 ICA may not develop OIS even with total occlusion of ICA.[24] Only 1 eye in our study developed OIS despite presence of thrombosis of OA in 10 eyes. Anatomical variation with limited ECA supply to the orbit and COVID-induced prothrombotic state have been cited as probable causes for OIS secondary to mucormycosis in a patient with COVID-19.[25] OIS did not manifest in the remaining 9 cases possibly due to good collateral circulation.

Cortical watershed infarcts occur at the border between cerebral vascular territories because of hypoperfusion and/or microemboli.[26] Though ICA narrowing/thrombosis was seen in 6 cases, cortical watershed infarcts were seen on MRI in only 2 cases.

The limitations of our study were inability to perform ocular fluorescein angiography, visually evoked response, carotid doppler, and magnetic resonance time of flight angiography in all the patients due to logistic restraints during the ongoing pandemic.

To conclude, in ROCM with orbital apex involvement, thrombotic ischemia of OA is a frequent accompaniment, presenting as acute visual loss. MR sequences are the preferred imaging modality for ascertaining the extent of soft tissue and vascular invasion by the fungus. Reduction of OA-PSV on color doppler imaging can serve as a sign of impending ocular ischemia, in cases with orbital apex involvement and absence of other factors likely to affect blood flow. Color doppler of OA and CRA can be employed as an adjunctive tool for diagnosis and monitoring of vascular occlusion in the event of nonvisualization of fundus or nonavailability of MR angiography.

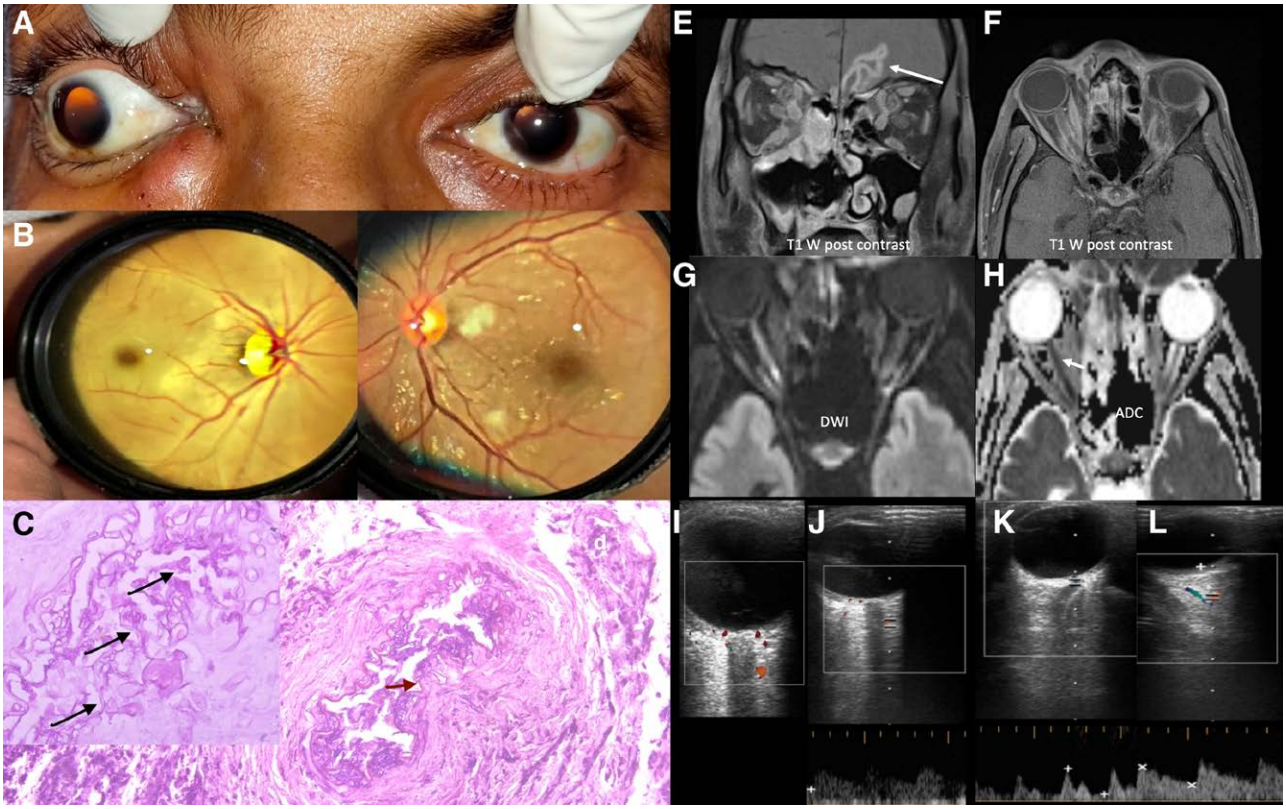

FIG. 5. **A**, Clinical photograph shows right periorbital abscess with partial ophthalmoplegia of both eyes. Fundus photograph (**B**) central retinal artery occlusion in right eye (**C**) cotton wool spots and arterial attenuation in left eye (**D**) histopathology of right exenterated orbit shows extensive necrosis and entrapped ophthalmic artery (OA) with fungal angioinvasion (Hematoxylin & Eosin - HE, 100×). Inset shows fungal hyphae highlighted by PAS stain (600×). T1-weighted postcontrast MRI depicts disease extending into both the orbits and accompanying left frontal lobe with a rim enhancing fungal abscess (**E**) coronal view, (**F**) axial view MRI, (**G**) diffusion-weighted imaging depicts bright signal on diffusion-weighted imaging. **H**, Corresponding drop of signal on ADC map of the right optic nerve suggesting diffusion restriction. Doppler ultrasonography shows peak systolic velocity of (**I**) 0 cm/s in right CRA, (**J**) 8.83 cm/s in right OA, (**K**) 8.11 cm/s in left CRA, (**L**) 9.55 cm/s in left OA.

ACKNOWLEDGMENTS

Funding support: nil
Financial disclosures: nil
Other acknowledgements: nill

REFERENCES

1. Sen M, Honavar SG, Bansal R, et al.; members of the Collaborative OPAI-IJO Study on Mucormycosis in COVID-19 (COSMIC) Study Group. Epidemiology, clinical profile, management, and outcome of COVID-19-associated rhino-orbital-cerebral mucormycosis in 2826 patients in India - Collaborative OPAI-IJO Study on Mucormycosis in COVID-19 (COSMIC), Report 1. *Indian J Ophthalmol* 2021;69:1670–1692.
2. Honavar SG. Code Mucor: guidelines for the diagnosis, staging and management of rhino-orbito-cerebral mucormycosis in the setting of COVID-19. *Indian J Ophthalmol* 2021;69:1361–1365.
3. Frank GS, Smith JM, Davies BW, et al. Ophthalmic manifestations and outcomes after cavernous sinus thrombosis in children. *J AAPOS* 2015;19:358–362.
4. Bae MS, Kim EJ, Lee KM, et al. Rapidly progressive rhino-orbito-cerebral mucormycosis complicated with unilateral internal carotid artery occlusion: a case report. *Neurointervention* 2012;7:45–49.
5. Song YM, Shin SY. Bilateral ophthalmic artery occlusion in rhino-orbito-cerebral mucormycosis. *Korean J Ophthalmol* 2008;22:66–69.
6. Luo QL, Orcutt JC, Seifter LS. Orbital mucormycosis with retinal and ciliary artery occlusions. *Br J Ophthalmol* 1989;73:680–683.
7. Al-Otaibi F, Albloushi M, Alhindi H, et al. Carotid artery occlusion by rhinoorbitocerebral mucormycosis. *Case Rep Surg* 2012;2012:812420.
8. Patil A, Mohanty HS, Kumar S, et al. Angioinvasive rhinocerebral mucormycosis with complete unilateral thrombosis of internal carotid artery-case report and review of literature. *BJR Case Rep* 2016;2:20150448.
9. Ferry AP, Abedi S. Diagnosis and management of rhino-orbito-cerebral mucormycosis (phycomycosis). A report of 16 personally observed cases. *Ophthalmology* 1983;90:1096–1104.
10. Downie JA, Francis IC, Arnold JJ, et al. Sudden blindness and total ophthalmoplegia in mucormycosis. A clinicopathological correlation. *J Clin Neuroophthalmol* 1993;13:27–34.
11. Mathur S, Karimi A, Mafee MF. Acute optic nerve infarction demonstrated by diffusion-weighted imaging in a case of rhinocerebral mucormycosis. *AJNR Am J Neuroradiol* 2007;28:489–490.
12. Badakere A, Patil-Chhablani P. Orbital Apex Syndrome: a review. *Eye Brain* 2019;11:63–72.
13. Alsuhaibani AH, Al-Thubaiti G, Al Badr FB. Optic nerve thickening and infarction as the first evidence of orbital involvement with mucormycosis. *Middle East Afr J Ophthalmol* 2012;19:340–342.
14. Kohn R, Hepler R. Management of limited rhino-orbital mucormycosis without exenteration. *Ophthalmology* 1985;92:1440–1444.
15. Sarkies N. Traumatic optic neuropathy. *Eye (Lond)* 2004;18:1122–1125.
16. Flaxel CJ, Adelman RA, Bailey ST, et al. Retinal and ophthalmic artery occlusions preferred practice pattern®. *Ophthalmology* 2020;127:P259–P287.

17. Bodanapally UK, Shanmuganathan K, Shin RK, et al. Hyperintense optic nerve due to diffusion restriction: diffusion-weighted imaging in traumatic optic neuropathy. *AJNR Am J Neuroradiol* 2015;36:1536–1541.
18. Groppo ER, El-Sayed IH, Aiken AH, et al. Computed tomography and magnetic resonance imaging characteristics of acute invasive fungal sinusitis. *Arch Otolaryngol Head Neck Surg* 2011;137:1005–1010.
19. Howells RC, Ramadan HH. Usefulness of computed tomography and magnetic resonance in fulminant invasive fungal rhinosinusitis. *Am J Rhinol* 2001;15:255–261.
20. Kim JH, Kang BC, Lee JH, et al. The prognostic value of gadolinium-enhanced magnetic resonance imaging in acute invasive fungal rhinosinusitis. *J Infect* 2015;70:88–95.
21. Kalin-Hajdu E, Hirabayashi KE, Vagefi MR, et al. Invasive fungal sinusitis: treatment of the orbit. *Curr Opin Ophthalmol* 2017;28:522–533.
22. Ashraf DC, Idowu OO, Hirabayashi KE, et al. Outcomes of a modified treatment ladder algorithm using retrobulbar amphotericin B for invasive fungal rhino-orbital sinusitis. Am J Ophthalmol 2021. doi:10.1016/j.ajo.2021.05.025
23. Brown GC, Magargal LE. The ocular ischemic syndrome. Clinical, fluorescein angiographic and carotid angiographic features. *Int Ophthalmol* 1988;11:239–251.
24. Terelak-Borys B, Skonieczna K, Grabska-Liberek I. Ocular ischemic syndrome - a systematic review. *Med Sci Monit* 2012;18:RA138–RA144.
25. Rao R, Shetty AP, Nagesh CP. Orbital infarction syndrome secondary to rhino-orbital mucormycosis in a case of COVID-19: clinico-radiological features. *Indian J Ophthalmol* 2021;69:1627–1630.
26. Momjian-Mayor I, Baron JC. The pathophysiology of watershed infarction in internal carotid artery disease: review of cerebral perfusion studies. *Stroke* 2005;36:567–577.

